

# Semiconductor band alignment from first principles: a new nonequilibrium Green's function method applied to the CZTSe/CdS interface for photovoltaics.

Mattias L. N. Palsgaard<sup>\*†</sup>, Andrea Crovetto<sup>†</sup>, Tue Gunst<sup>†</sup>, Troels Markussen<sup>\*</sup>, Ole Hansen<sup>†</sup>, Kurt Stokbro<sup>\*</sup>  
and Mads Brandbyge<sup>†</sup>

<sup>†</sup>Center for Nanostructured Graphene (CNG), Department of Micro- and Nanotechnology (DTU Nanotech)

<sup>\*</sup>Quantumwise A/S, Fruebjergvej 3, Postbox 4, DK-2100 Copenhagen, Denmark

**Abstract**—In this paper we present a method to obtain the band offset of semiconductor heterointerfaces from Density Functional Theory together with the nonequilibrium Green's function method. Band alignment and detailed properties of the interface between  $\text{Cu}_2\text{ZnSnSe}_4$  and CdS are extracted directly from first principles simulations. The interface is important for photovoltaics applications where in particular the band offsets are important for efficiency. The band bending pose a problem for accurate atomistic simulations of band offsets due to its long range. Here we investigate two different methods for dealing with band bending directly. One involves doping the materials to induce a shorter screening length. The other method is to apply a voltage bias across the interface to correct for the band bending. The calculated band offsets agree well with previous experimental and theoretical studies and, interestingly, the offset is seen to depend on whether or not the interface is under flat-band conditions.

## I. INTRODUCTION

Semiconductor heterointerfaces play an increasingly important role in optical and electronic devices due to miniaturization and to the pervasive trend of introducing new materials to tailor the desired device properties [1]. In particular, the valence- and conduction band offsets (VBO and CBO) at the interface affect the transport properties and recombination rates at the interface [2].

Methods to obtain VBO and CBO from first principles have been recently reviewed [3]. Among them, an explicit interface modeling method inspired by the photoemission measurement has gained significant popularity due to its excellent agreement with experimental data [4]–[6]. In this method, the energy positions of the valence bands of materials A and B are first calculated separately in the two unstrained bulk materials with respect to a reference energy unique to each bulk calculation (for example, the position of a core level). Then, an explicit interface calculation is employed to align the two valence band positions to a common energy reference, which can be a core level or the averaged local potential.

Conversely, we propose a method where the band alignment can be obtained directly from the interface supercell

calculation containing both materials using Density Functional Theory (DFT) together with Nonequilibrium Green's functions (NEGF). In this way it is further possible to extract information about the atomic properties of the interface such as defects and tunneling of states over the interface and study transport phenomena. Similar methods have been used previously to study Schottky barriers [7].

To demonstrate this method, we have selected the CZTSe-CdS interface as a case study.  $\text{Cu}_2\text{ZnSnSe}_4$  (CZTSe, band gap 1.0 eV),  $\text{Cu}_2\text{ZnSnS}_4$  (CZTS, band gap 1.5 eV) and their alloy  $\text{Cu}_2\text{ZnSnS}_x\text{Se}_{4-x}$  (CZTSSe, tunable band gap 1.0–1.5 eV) are promising p-type semiconductors for thin-film photovoltaics. To indicate all three materials in general terms we use the notation CZTS(e). In solar cell devices, their n-type heterojunction partner is typically CdS, with which the best conversion efficiencies reported so far have been achieved [8], [9]. A schematic band diagram is shown in Fig. 1(a).

As noted in a number of review papers [10]–[12], loss mechanisms at the CZTS(e)/CdS interface are believed to be one of the reasons why laboratory-scale CZTS(e) solar cells still lag far behind their theoretical maximum efficiency. To emphasize the potentially dramatic consequences of an unfavorable band alignment of the CZTSe/CdS interface on solar cell efficiency, we have carried out a device-level simulation (Fig. 1(b)). There, we have swept the electron affinity of CZTSe to recreate different hypothetical band alignments, according to Anderson's rule [2]. The results are shown in Fig. 1(b). A type I alignment, or conduction band "spike" with a height between +0.1 eV and +0.4 eV (Fig. 1) is found to be optimal, in agreement with similar studies on other solar cell heterointerfaces [13], [14].

Despite the importance of the offset values in device performance, only few reports of calculated band alignments are available in the literature and mostly with focus on CZTS. Only one report could be found on CZTSe [15]. To the best of our knowledge, only the photoemission-inspired calculation method [4] has been reported for any CZTS(e)/CdS interface [15]. The actual band alignment at the CZTS-CdS interface is still disputed, with experimental and theoretical offsets scat-

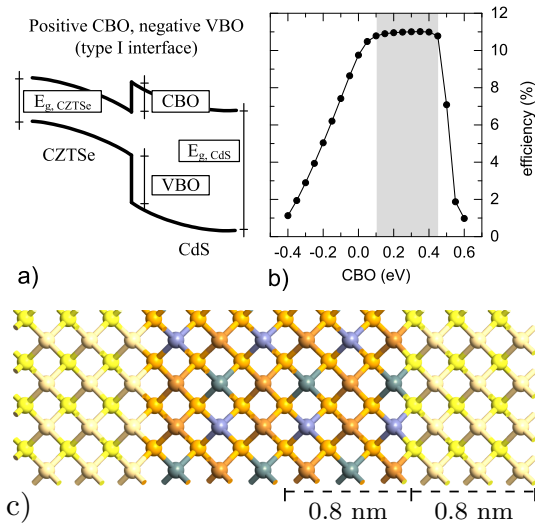


Figure 1: a) Schematic illustration of the sign conventions and symbols used for the band alignment problem. The signs of the CBO and VBO are referred to the lower band gap semiconductor, so that a positive CBO means that the CdS conduction band lies above the CZTSe conduction band. Assuming a negative VBO, a positive (negative) CBO results in a type I (II) interface, also known as conduction band spike (cliff).  $E_{g,CZTSe}$  and  $E_{g,CdS}$  are the band gaps of CZTSe and CdS respectively. b) Simulated CZTSe/CdS heterojunction solar cell efficiency as a function of the conduction band offset. The shaded region is the optimal CBO range for achieving maximum efficiency. c) Periodic supercell containing the (100)/(100) interface of CZTS and CdS, dimensioned as in previously reported calculations [15].

tered in a broad energy range -0.34 eV to +0.45 eV. However, the few existing studies for the CZTSe-CdS interface are in rather good agreement: Different photoemission experiments have measured +0.48 eV [16], +0.34 eV [17], and +0.3 eV offsets [18], while a theoretical study has calculated a +0.34 eV offset [15]. This provides a benchmark for our proposed method and allows adding new information to an interface in which the band alignment is relatively well established.

## II. COMPUTATIONAL DETAILS

The preliminary device-level simulation was performed numerically with the finite-element method as implemented in the thin-film solar cell simulation software SCAPS [19] on a standard CZTSe/CdS/ZnO device structure. The material parameters were taken from various literature sources [20], [21]. The CBO between CZTSe and CdS was swept from -0.4 eV to +0.6 eV by sweeping the electron affinity of CZTS while maintaining the flat band conditions at the contacts.

All first-principles calculations in this study were performed with the ATK DFT software [22] using a double zeta polarized LCAO basis set [23], [24]. The combination of DFT with NEGF enables a device setup with semi-infinite electrodes on each side of the interface.

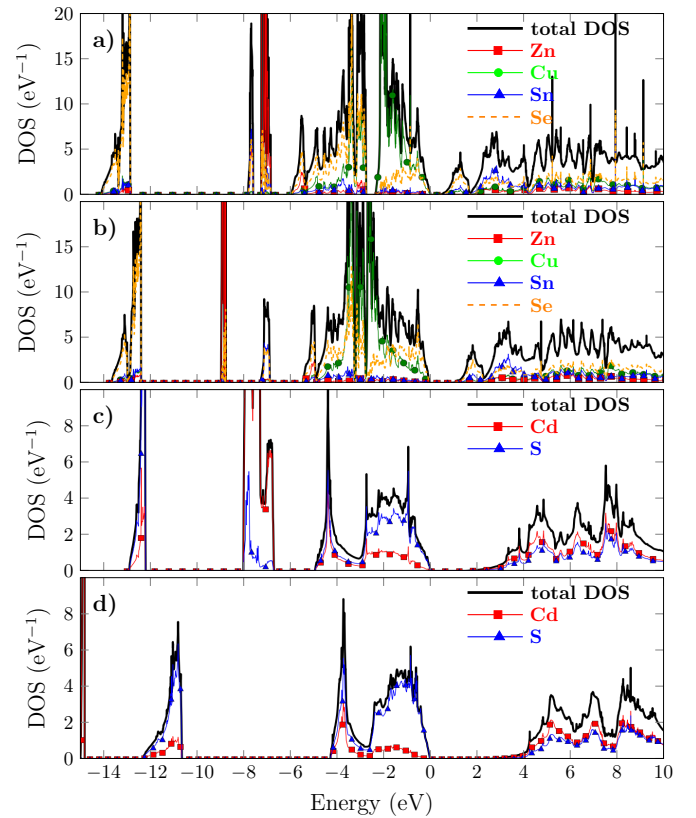


Figure 2: Total and projected density of states of bulk CZTSe calculated with GGA (a) and GGA + U (b) and for bulk CdS calculated with GGA (c) and GGA + U (d).

It is well known that the bandgaps of CZTSe and CdS are poorly reproduced with the conventional local density approximation (LDA) or generalized gradient approximation (GGA) approach to the exchange-correlation potential in DFT calculations [15]. We use the semi-empirical Hubbard correction where an additional energy term of the form

$$E_U = \frac{1}{2} \sum_{\mu} U_{\mu} (n_{\mu} - n_{\mu}^2) \quad (1)$$

where  $n_{\mu}$  is the projection onto an atomic shell and  $U$  is chosen to reproduce the experimental bandgap in the bulk unit cell of either material, is added to the usual GGA-PBE exchange-correlation functional. This method is a computationally cheap way to correct for the self interaction of localized electrons in strongly correlated systems [25]. In Fig. 2, we compare density of states (DOS) of bulk CZTSe calculated with and without the Hubbard correction term. As expected the bandgaps are opened and the valence bands of d-like character for Zn and Cd are downshifted in energy. This is very similar to the effects seen when using the  $G_0W_0$ (HSE) approach on CZTS [26] indicating a high degree of self interaction error in these systems. Previous theoretical studies [15] have been performed on interface supercells with up to 3 unit cells of either material. This means that dimensions only up to a few nm in the direction perpendicular to the interface plane have been used

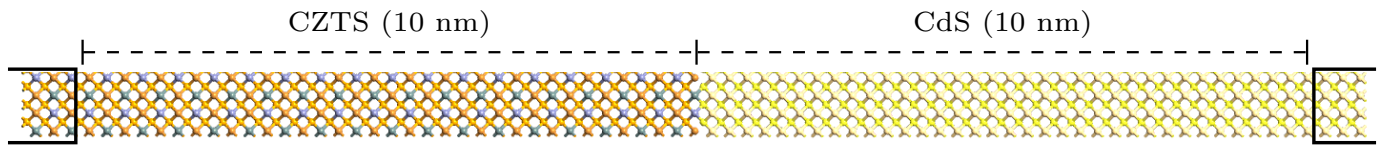


Figure 3: Structure used to simulate the 100/100 interface of CZTSe (left) and CdS (right). The supercell is more than five times larger than that used in previous work [15].

(Fig. 1). Furthermore these calculations were performed using periodic boundary conditions (PBC) in all directions resulting in interfaces separated by less than 2 nm as shown in Fig. 1.

Instead, in this work we employed a supercell that is 20 nm in length (Fig. 3) and semi-infinite boundary conditions in the direction perpendicular to the interface plane, as allowed by the DFT-NEGF approach. This assures that bulk-like conditions are met on either side. This approach can be justified as the thickness of each layer of material in real devices is tens of nm for CdS and hundreds of nm for CZTSe, so semi-infinite boundary conditions give a better description of the situation than PBC's [7]. The supercells employed in the calculation are periodic along the interface using  $5 \times 3$  k-points. In the electrodes of the device a  $3 \times 5 \times 100$  k-point grid is used. K-points were chosen so that the total energy of the bulk materials was converged to within 0.5 meV. Several interfaces can be constructed with different surface geometries and formation energies. Here we consider the CZTSe(100)/CdS(100) interface, which has relatively low strain of  $\sim 2.5\%$ . GGA + U is known to overestimate lattice parameters for CZTSe, we therefore keep the experimental lattice parameter for CZTSe. When setting up the interface the CdS bulk crystal is strained to fit that of CZTSe.

All relaxation were performed until interatomic force were below  $0.02 \text{ eV}/\text{\AA}$ . Calculations of the local density of states (LDOS) in the device were performed using  $11 \times 11$  k-points. Using this scheme we can for the first time study directly the effect of the interface on the band-alignment and transport properties in this system.

### III. RESULTS

Fig. 4(a) shows the LDOS and the local potential across the intrinsic (non-doped) interface. We see a clear spike-like CBO in agreement with previous theoretical and experimental studies [15], [16]. The potential shows a residual slope towards the electrodes indicating that the screening is not contained within the supercell. Nevertheless, the CBO obtained with this method ( $\sim 0.3 \text{ eV}$ ) is in good agreement with experimental data measured under equilibrium conditions [17], [18]. To address the problem of the residual slope in the potential, one can reduce the screening length by doping both materials. Our simulations include doping by adding a complementary charge to the atomic sites. Fig. 4(b) shows the LDOS and local potential across the interface where a p-type (n-type) charge density of  $10^{18} \text{ cm}^{-3}$  unit charges are added to CZTSe (CdS). Adding the charge removes the residual slope of the potential, however it also dramatically changes the electronic structure of

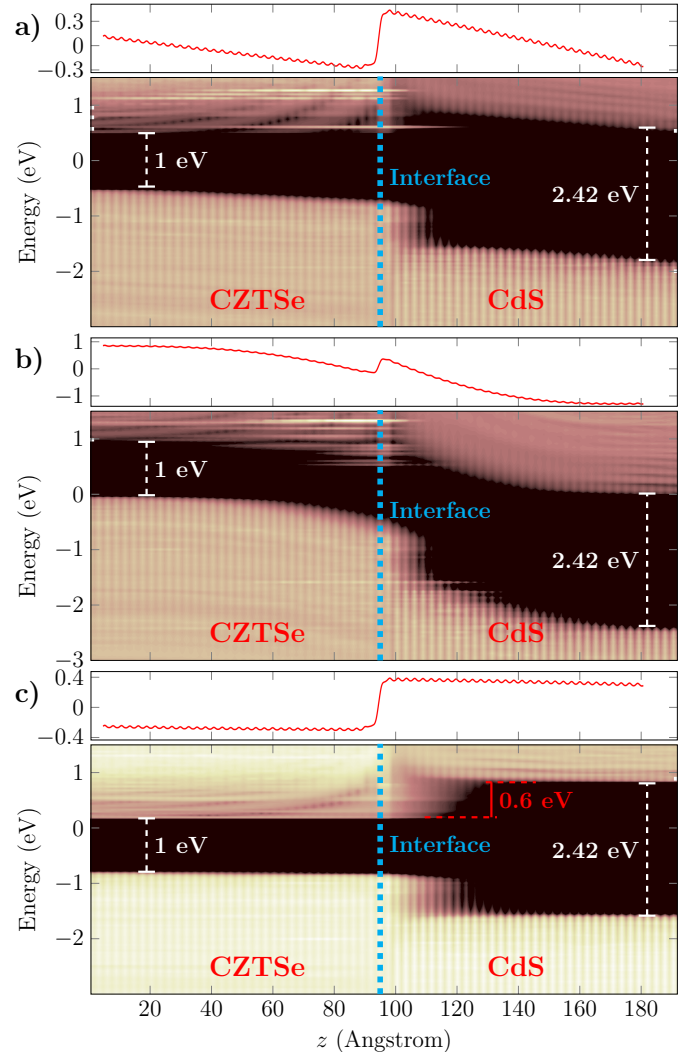


Figure 4: The local potential (top) and local density of states (bottom) of the CZTSe/CdS interface resolved along the direction perpendicular to the interface surface. (a) equilibrium conditions with zero bias and zero doping; (b) equilibrium conditions with zero bias and  $10^{18} \text{ cm}^{-3}$  doping density; (c) non-equilibrium conditions with an applied forward bias to achieve flat-band conditions and zero doping.

the interface. Further, it must be emphasized that the amount of charge needed here to contain the screening within the cell is very large compared to the real doping density of CZTSe, which is on the order of  $10^{15} - 10^{16} \text{ cm}^{-3}$  [8]. In

fact, the experimental screening length of CZTSe (equivalent to the depletion region width in a p-n<sup>+</sup> junction device) is about 20 times larger than the width of the CZTSe layer in our supercell and consequently several hundred times larger than previous theoretical studies [8], [15]. To handle weakly screened materials, i.e. with band bending occurring over more than a few nm, we apply a small forward bias in the device simulations. Fig. 4(c) shows the LDOS and potential across such a system. Clearly we have in this way achieved flat band conditions on both sides of the device and at the same time removed the residual slope of the local potential. Such a calculation is only possible due to the device setup we have used here. The obtained CBO is +0.6 eV which agrees nicely with the only reported measurement done under flat-band conditions [16]. Note that the CBO is larger in the flat-band case than in the case of equilibrium band bending, which was also the case in experimental studies [16]–[18]. Finally in the LDOS for the undoped and doped systems at equilibrium, Fig. 4(a) and Fig. 4(b) respectively, localized states appear inside the gaps of either material. Localized states can have a crucial impact on the performance of any electronic device by e.g. increasing the recombination rate. They may also lead to errors in experimental measurements of band offsets due to lack of sufficient resolution to distinguish an interface state from its nearest bulk band. These states can be addressed directly in the device method as opposed to bulk supercell simulations. In particular, we note that the CBO in the doped system (Fig. 4(b)) is strongly influenced by the presence of localized states.

#### IV. CONCLUSION

We have successfully analyzed the electronic structure of the interface between CdS and Cu<sub>2</sub>ZnSnSe<sub>4</sub> using first principles calculations. This interface is of particular interest for the photovoltaics community. The conduction band offset across the interface has been identified as a bottleneck for efficiency of a promising thin-film solar cell device, using device simulations. From DFT-NEGF calculations a CBO of +0.6 eV is found under flat-band conditions imposed by applying a forward bias over the interface to correct for band-bending. The results agree reasonably well with experiments under equilibrium and flat-band conditions.

#### ACKNOWLEDGMENT

This work is partly funded by the Innovation Fund Denmark (IFD) under File No. 5016-00102.

#### REFERENCES

- [1] "The interface is still the device." *Nature materials*, vol. 11, no. 2, p. 91, mar 2012.
- [2] G. Margaritondo, *Electronic structure of semiconductor heterojunctions*. Kluwer Academic Publishers.
- [3] Y. Hinuma, A. Grüneis, G. Kresse, and F. Oba, "Band alignment of semiconductors from density-functional theory and many-body perturbation theory," *Physical Review B*, vol. 90, no. 15, p. 155405, oct 2014.
- [4] S.-H. Wei and A. Zunger, "Calculated natural band offsets of all II–VI and III–V semiconductors: Chemical trends and the role of cation d orbitals," *Applied Physics Letters*, vol. 72, no. 16, p. 2011, apr 1998.
- [5] A. Alkauskas, P. Broqvist, F. Devynck, and A. Pasquarello, "Band Offsets at Semiconductor-Oxide Interfaces from Hybrid Density-Functional Calculations," *Physical Review Letters*, vol. 101, no. 10, p. 106802, sep 2008.
- [6] Y.-H. Li, A. Walsh, S. Chen, W.-J. Yin, J.-H. Yang, J. Li, J. L. F. Da Silva, X. G. Gong, and S.-H. Wei, "Revised ab initio natural band offsets of all group IV, II–VI, and III–V semiconductors," *Applied Physics Letters*, vol. 94, no. 21, p. 212109, may 2009.
- [7] D. Stradi, U. Martinez, A. Blom, M. Brandbyge, and K. Stokbro, "General atomistic approach for modeling metal-semiconductor interfaces using density functional theory and nonequilibrium green's function," *Phys. Rev. B*, vol. 93, p. 155302, Apr 2016.
- [8] Y. S. Lee, T. Gershon, O. Gunawan, T. K. Todorov, T. Gokmen, Y. Virgus, and S. Guha, "Cu<sub>2</sub>ZnSnSe<sub>4</sub> Thin-Film Solar Cells by Thermal Co-evaporation with 11.6% Efficiency and Improved Minority Carrier Diffusion Length," *Advanced Energy Materials*, vol. 5, no. 7, p. 1401372, apr 2015.
- [9] W. Wang, M. T. Winkler, O. Gunawan, T. Gokmen, T. K. Todorov, Y. Zhu, and D. B. Mitzi, "Device Characteristics of CZTSSe Thin-Film Solar Cells with 12.6% Efficiency," *Advanced Energy Materials*, vol. 4, no. 7, p. 1301465, nov 2013.
- [10] S. Siebentritt, "Why are kesterite solar cells not 20% efficient?" *Thin Solid Films*, vol. 535, pp. 1–4, 2013.
- [11] A. Polizzotti, I. L. Repins, R. Noufi, S.-H. Wei, and D. B. Mitzi, "The state and future prospects of kesterite photovoltaics," *Energy & Environmental Science*, vol. 6, no. 11, pp. 3171–3182, oct 2013.
- [12] X. Liu, Y. Feng, H. Cui, F. Liu, X. Hao, G. Conibeer, D. B. Mitzi, and M. Green, "The current status and future prospects of kesterite solar cells: a brief review," *Progress in Photovoltaics: Research and Applications*, jan 2016.
- [13] T. Minemoto, T. Matsui, H. Takakura, Y. Hamakawa, T. Negami, Y. Hashimoto, T. Uenoyama, and M. Kitagawa, "Theoretical analysis of the effect of conduction band offset of window/CIS layers on performance of CIS solar cells using device simulation," *Solar Energy Materials and Solar Cells*, vol. 67, no. 1, pp. 83–88, 2001.
- [14] M. Gloeckler and J. Sites, "Efficiency limitations for wide-band-gap chalcopyrite solar cells," *Thin Solid Films*, vol. 480–481, pp. 241–245, jun 2005.
- [15] S. Chen, A. Walsh, J.-H. Yang, X. G. Gong, L. Sun, P.-X. Yang, J.-H. Chu, and S.-H. Wei, "Compositional dependence of structural and electronic properties of Cu<sub>2</sub>ZnSn(S,Se)<sub>4</sub> alloys for thin film solar cells," *Physical Review B*, vol. 83, no. 12, p. 125201, mar 2011.
- [16] R. Haight, A. Barkhouse, O. Gunawan, B. Shin, M. Copel, M. Hopstaken, and D. B. Mitzi, "Band alignment at the Cu<sub>2</sub>ZnSn(S<sub>x</sub>Se<sub>1-x</sub>)<sub>4</sub>/CdS interface," *Applied Physics Letters*, vol. 98, no. 25, p. 253502, jun 2011.
- [17] J. Li, M. Wei, Q. Du, W. Liu, G. Jiang, and C. Zhu, "The band alignment at CdS/Cu<sub>2</sub>ZnSnSe<sub>4</sub> heterojunction interface," *Surface and Interface Analysis*, vol. 45, no. 2, pp. 682–684, feb 2013.
- [18] T. Kato, H. Hiroi, N. Sakai, and H. Sugimoto, "Buffer/Absorber Interface Study on Cu<sub>2</sub>ZnSnS<sub>4</sub> and Cu<sub>2</sub>ZnSnSe<sub>4</sub> Based Solar Cells: Band Alignment and Its Impact on the Solar Cell Performance." *28th European Photovoltaic Solar Energy Conference*, pp. 2125–2127, sep 2013.
- [19] M. Burgelman, P. Nollet, and S. Degraeve, "Modelling polycrystalline semiconductor solar cells," *Thin Solid Films*, vol. 361–362, pp. 527–532, feb 2000.
- [20] M. Gloeckler, "Device physics of Cu(In,Ga)Se<sub>2</sub> thin-film solar cells," PhD thesis, Colorado State University, 2005.
- [21] K. Ito, *Copper Zinc Tin Sulfide-Based Thin-Film Solar Cells*. Wiley, 2015.
- [22] Atomistix ToolKit version 2015.0, QuantumWise A/S.
- [23] J. M. Soler, E. Artacho, J. D. Gale, A. García, J. Junquera, P. Ordejón, and D. Sánchez-Portal, "The siesta method for ab initio order-n materials simulation," *Journal of Physics: Condensed Matter*, vol. 14, no. 11, p. 2745, 2002.
- [24] M. Brandbyge, J.-L. Mozos, P. Ordejón, J. Taylor, and K. Stokbro, "Density-functional method for nonequilibrium electron transport," *Phys. Rev. B*, vol. 65, p. 165401, Mar 2002.
- [25] V. I. Anisimov, J. Zaanen, and O. K. Andersen, "Band theory and Mott insulators: Hubbard U instead of Stoner I," *Physical Review B*, vol. 44, no. 3, pp. 943–954, jul 1991.
- [26] J. Paier, R. Asahi, A. Nagoya, and G. Kresse, "Cu<sub>2</sub>ZnSnS<sub>4</sub> as a potential photovoltaic material: A hybrid hartree-fock density functional theory study," *Phys. Rev. B*, vol. 79, p. 115126, Mar 2009.